Proceedings World Geothermal Congress 2026
Calgary, Canada, June 8 – 11, 2026

Origin of Critical Raw Minerals (CRM) in a Metamorphosed Flysch Geothermal System: A Case Study from Seferihisar, Western Anatolia

Alper Baba[1*], Tolga Ayzit[1], Franziska Wilke[2]; Martin Zimmer[2], Andri Stefánsson[3], Michael Bau[4], Lukas Klose[4], Katrin Kieling[2], Simona Regenspurg[2], Mustafa M. Demir[5]

[1]Izmir Institute of Technology, Department of International Water Resources, Urla, Izmir 35430, Türkiye

[2]GFZ German Research Centre for Geosciences, Potsdam, Germany

[3]Institute of Earth Sciences, University of Iceland, Sturlugata 7, 101 Reykjavík, Iceland

[4]School of Science, Constructor (formerly Jacobs) University Bremen gGmbH, Bremen, Germany

[5]Izmir Institute of Technology, Department of Material Science and Engineering, Urla, Izmir 35430, Türkiye

*alperbaba@iyte.edu.tr

Keywords: Geothermal Exploration, Hydrothermal Systems, Critical Raw Materials (CRM), Seferihisar Geothermal Field, Western Anatolia

INTRODUCTION

Critical raw minerals (CRM) are of interest in geothermal systems because certain elements essential for modern technologies, most notably lithium (Li) and boron (B), are mobilized and concentrated in geothermal fluids and related brines. This creates potential secondary resources that can be recovered alongside conventional energy production (IEA, 2024; Dini et al., 2022; Ettehadi et al., 2024; Rosen et al., 2020).

High-enthalpy geothermal systems are characterized by hot fluids (up to 250°C) and robust fluid flow through crystalline to metamorphosed crust, with fluids commonly enriched in CO_2 and dissolved solids. In western Anatolia, systems are reported to operate at medium to high enthalpy with alkaline-bicarbonate waters and substantial CO_2 contents. This indicates extensive fluid-rock interaction and mixing among deep-sourced hydrothermal fluids, meteoric input, and crustal CO_2 (Friðleifsson et al., 2020; Serpen et al., 2009). Metamorphosed flysch has been shown to host minerals and trace-element assemblages that (a) are inherently enriched in certain CRM candidates or (b) become mobilizable under high-temperature, high-salinity hydrothermal conditions (Konrad-Schmolke and Halama, 2014).

The present study evaluates the evidence-based explanation for why waters originating from metamorphosed flysch-associated, high-enthalpy geothermal systems can carry elevated contents of critical raw materials (CRMs) in the Seferihisar geothermal region, western Anatolia.

METHODS & RESULTS

Samples of chips were obtained from a production well located in a local expansion zone, exhibiting metamorphosed flysch reservoir rock and an outflow temperature of 140°C, extending to a depth of 1,400 meters (Figure 1). Whole rock analyses of major and trace elements were performed using X-ray fluorescence (XRF spectrometer), and trace elements (especially CRM) were determined by inductively coupled plasma mass spectrometry (ICP-MS). Detailed mineral analyses were conducted using X-ray diffraction (XRD).

The basement in Seferihisar is characterized by the prevalence of the Paleozoic Menderes Massif and the Cretaceous Bornova Melange. The Menderes Massif consists of various schists interbedded with marble lenses. The Bornova Melange is composed of blocks of limestone, chert, submarine volcanics, and serpentinites embedded in a flysch matrix, which consists of alternating sandstone and shale. During the Neogene period, sandstone formed within various alluvial fan and lacustrine fan deltaic conglomerates, which are associated with extensional tectonic regimes. The extensional tectonics of western Anatolia facilitate the circulation of fluids at depth and the transport of fluids from deep volcanic or metasomatic sources to higher levels, controlled by faulting. Serpentinite and spilite form a transition zone associated with deep reactive environments. Both were formed when ultramafic rocks and basaltic lavas, respectively, reacted with seawater or with hydrothermal fluids derived from circulating seawater through hot volcanic rocks.

In the Seferihisar geothermal field, energy is produced from geothermal wells at depths of 2,200 m and 265 m. The temperatures of these wells are 170°C and 140°C, respectively. Comprehensive elemental measurements were conducted on collected water samples, revealing concentrations of B (19 ppm), Li (14 ppm), Rb (7.1 ppm),

and Cs (2.4 ppm). Additionally, scale samples from the site contained Sr (547 ppm), Pb (233.79 ppm), Zn (392.99 ppm), Ag (19.77 ppm), Rb (11.19 ppm), and Cs (9.26 ppm).

The 265 m well intersects conglomerate and spilite lithologies, while the 2,200 m well intersects conglomerate, spilite, metamorphosed flysch, serpentinite, and schist lithologies. ICP-MS analysis of chip samples from the site shows Sr (110 ppm) and Cu (180 ppm) in conglomerate samples. As the investigation progresses, the concentrations of Pb (207 ppm), Cs (3.27 ppm), Rb (20.71 ppm), Zn (337 ppm), and As (250 ppm) in metamorphosed flysch are of particular interest. Finally, the serpentinite and shale rocks that form the base rock contain Ag (58.94 ppm), Ni (1,269 ppm), Co (116 ppm), and Cr (2,618 ppm) (Figure 2).

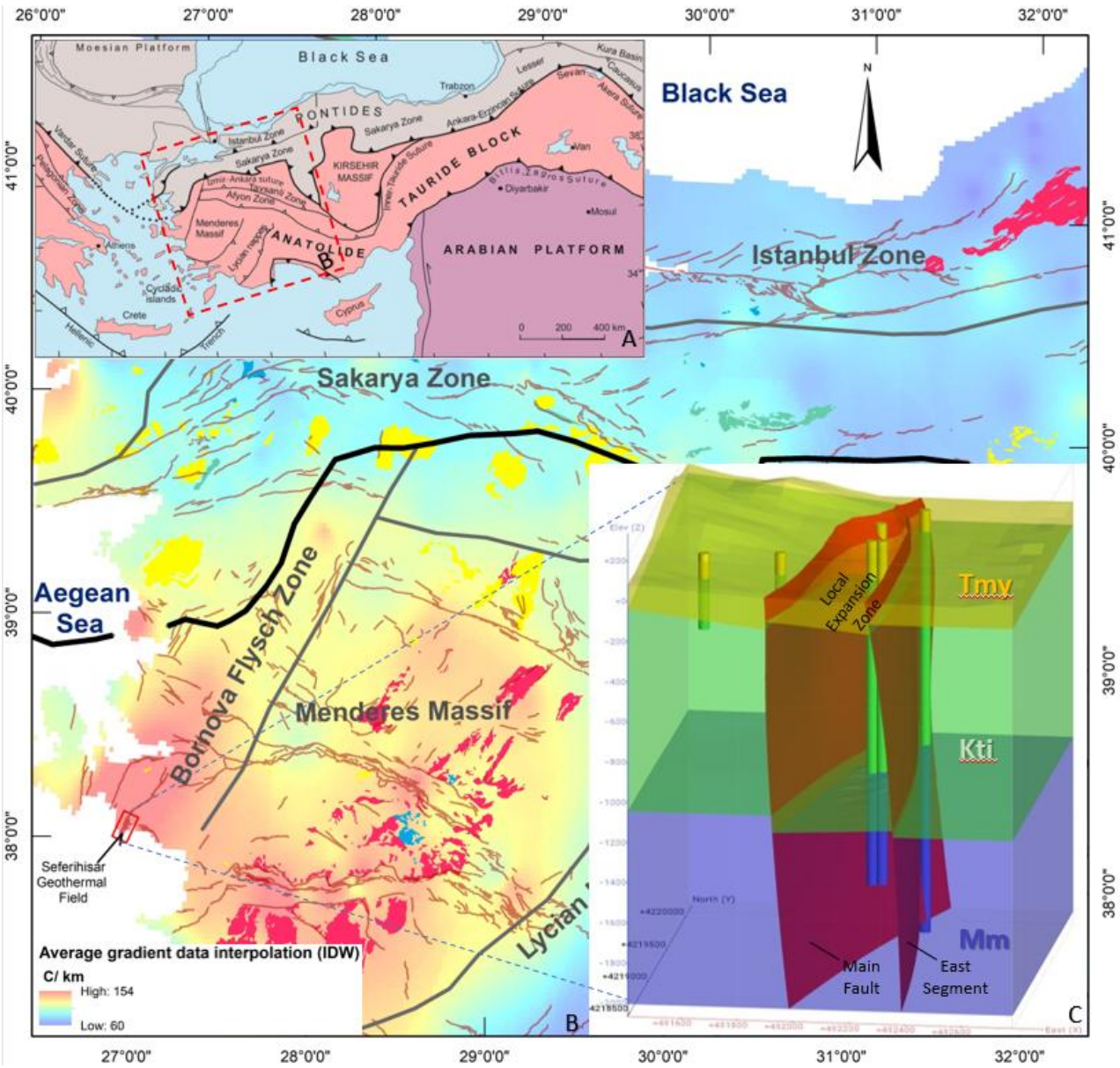


Figure 1. A) Tectonic map of Türkiye (Okay and Tüysüz, 1999) B) Gradient data interpolation map of western Anatolia (IDW: Inverse Weighted Distance) Modified from (Ayzit et al., 2025) C) Conceptual model of Seferihisar Geothermal Field. Tmy: Alluvial fan and lacustrine fan deltaic conglomerate, sandstone; Kti : Izmir flysch (blocked flysch): Matrix; mudstone, sandstone, limestone, conglomerate & spilite; Mm: Menderes massif. Main fault: N05E/81NW, East segment: N15E/87NW

XRD analyses of the drill core samples, covering depths from the surface to 1400 m, reveal distinct vertical mineralogical zonation (Table 1). The near-surface intervals (0–200 m) are characterized by abundant carbonates (calcite, dolomite, ankerite, magnesite, siderite) and significant quartz, indicating widespread hydrothermal alteration that has overprinted the host lithology. Accessory aluminosilicates (albite, muscovite,

biotite, phengite, paragonite) are present in these upper levels, consistent with the stability of low- to medium-grade phyllosilicates.

Between 200and 800 m, the mineral assemblage is enriched in phyllosilicates (chlorite group, chamosite, clinochlore, amesite), along with pyroxenes (enstatite, ferrosilite, augite) and tourmaline-group minerals (dravite). The occurrence of sporadic staurolite, axinite, and hiortdahlite in the examined area suggests increasing metamorphic and hydrothermal influences at depth.

Below 800 m, there is a transition in mineralogy toward a greater prevalence of critical raw material (CRM)-bearing phases, including spodumene (Li source), lithiophorite (Li–Mn hydroxide), birnessite (Mn oxide), and villamaninite (Ni–Co sulfide) (Figure 3). Associated phases, such as chalcocite (Cu_2S), tenorite (CuO), wüstite (FeO), and ramdohrite (Pb–Ag sulfosalt), indicate sulfide mineralization horizons. Rare but significant occurrences of zirconium oxide (ZrO_2) and zippeite (uranium sulfate) have also been documented, especially at the deepest intervals (1000–1400 m)).

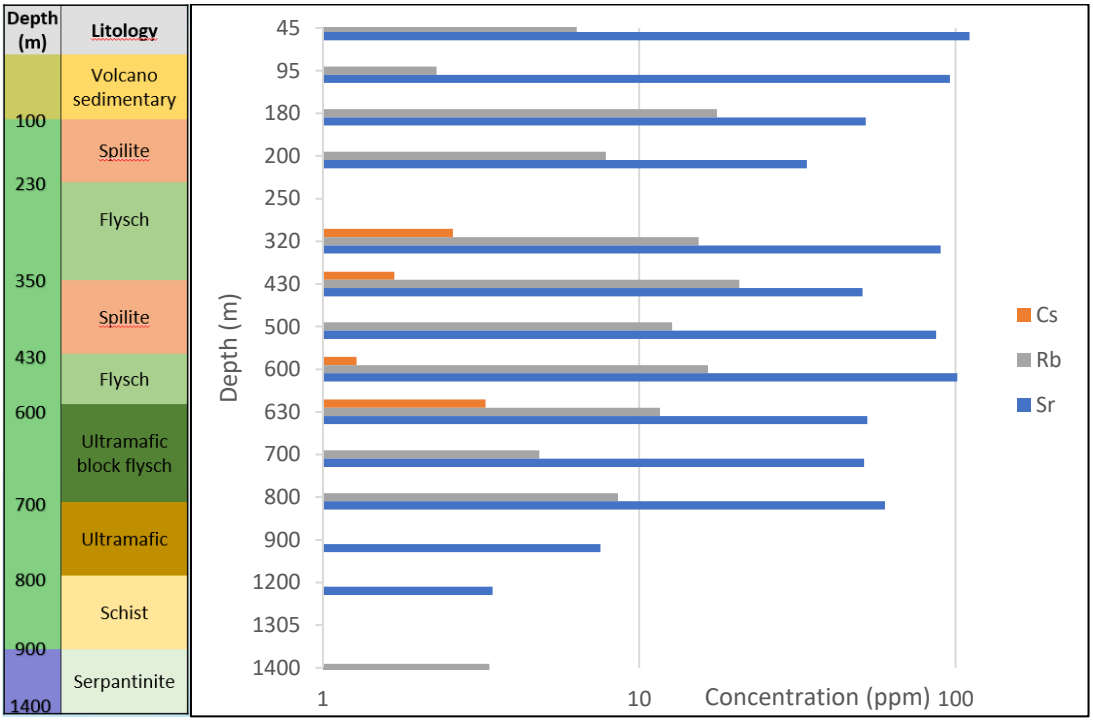


Figure 2. Litostratigraphic column section and the depth-dependent Sr, Rb and Cs concentrations

DISCUSSION & CONCLUSION

Spodumene ($LiAlSi_2O_6$) and lithiophorite, which contain lithium, are direct lithium reservoirs; additionally, alkali feldspars, mica, and pegmatitic phases (e.g., altered zones within albite, lepidolite-like phases, or pegmatite fragments) are sources of lithium. Spodumene-pegmatites and albite-spodumene systems can be enriched in lithium through magmatic-hydrothermal processes (Chen et al., 2022). As large-ion alkali metals, mica (muscovite, phengite, biotite, phlogopite) and alkali feldspars/K-feldspar can substitute for each other; therefore, the mica/feldspar potential in the rock indicates the Rb-Cs source (Icenhower and London, 1996).

Li becomes highly mobile, especially in hot, high-Cl aqueous solutions (brineor magmatic-hydrothermal fluids). Li–Cl complexes provide transport in the fluid; thus, high temperature and high salinity increase Li mobilization. Rb and Cs also migrate in the fluid with temperature, but these elements dissolve primarily from mica and K-phases (Gourcerol et al., 2024). During smectite/illite conversion, Li (and K, Rb, Cs) can be released into the fluid, or under certain conditions, illite can retain Li. However, the literature indicates that hydrolytic illitization is a strong Li-trapping mechanism and that Li can become enriched within chlorite, illite, or both. This is a key process for both the release and re-trapping of Li in deep, high-temperature hydrothermal zones (Benson et al., 2023).

In closed systems (slow-flowing, high salinity) or evaporative/concentration zones, Li, Rb, and Cs can accumulate in the liquid phase. Concurrently, Mn-oxides/hydroxides (e.g., birnessite, lithiophorite) can retain elements through precipitationor filtration on their surfaces or in colloids. Consequently, Mn-oxide zones can function as a 'sorption' or secondary accumulation surface for both Li and Cs (Gourcerol et al., 2024).

In conclusion, the study demonstrates that high fluid-phase CRM concentrations indicate deep crustal sourcing and efficient mobilization by geothermal circulation. The solid-phase accumulation of CRM in serpentinites, spilites, and flysch reservoirs indicates prolonged hydrothermal alteration and metal transport.

Table 1. XRD analyses of the drill core samples, covering depths from the surface down to 1400 m

Depth(m)	Compound name of Quantification (%)										Dominant zone
	10	20	30	40	50	60	70	80	90	100	
45	Quartz		Ankerite				Siderite	Magnesite	Villamaninite		Quartz-calcite
95	Albite				Dolomite		Magnesite		Calcite	Quartz	Carbonate-albite-mica
180	Quartz						Phengite			Dolomite	
200	Lithium l-tartrate				Dolomite		Ramdohrite	Paragonite	Li Propanoate	CsRbTiOAsO4	
250	Albite			Antipyrine-aminobenzoic acid	Dolomite		Quartz		Cs Ti oxide arsenate	Li phythalocyanine chloride	Smectite/illite transition zone
320	Quartz			Albite				Chamosite		Li phythalocyanine chloride	
430	Quartz		Dolomite	Ankerite	Muscovite				Clinoenstatite		
500	Quartz	Dolomite	Calcite	Muscovite							
600	Quartz			Dolomite		Calcite	Gibbsite	Nepheline	Biotite		Clorite-proxene-tourmaline (prograde alteration)
630	Dolomite		Albite				Mo32Cs4P16O132		Hiortdahlite I		
700	Albite		Dravite		Mn axinite				Staurolite		
800	Quartz		Clinochlore		Phlogopite		Ferrosilite	Enstatite	Chamosite	Calcite	Li-CRM zone
900	Albite		Chlorite				Lithiophorite	Li phthalocyanine chloride		Spodumene	
1200	Birnessite		Friedelite					Zippeite	Amesite		Sulfide- ZrO_2- zippeite (multi-stage mineralization)
1305	Zirconium Oxide tetragonal		Birnessite			Wuestite	Pertsevite	Chalcocite			
1400	Tenorite		Fe tetraborate		Jasmundite		Augite				

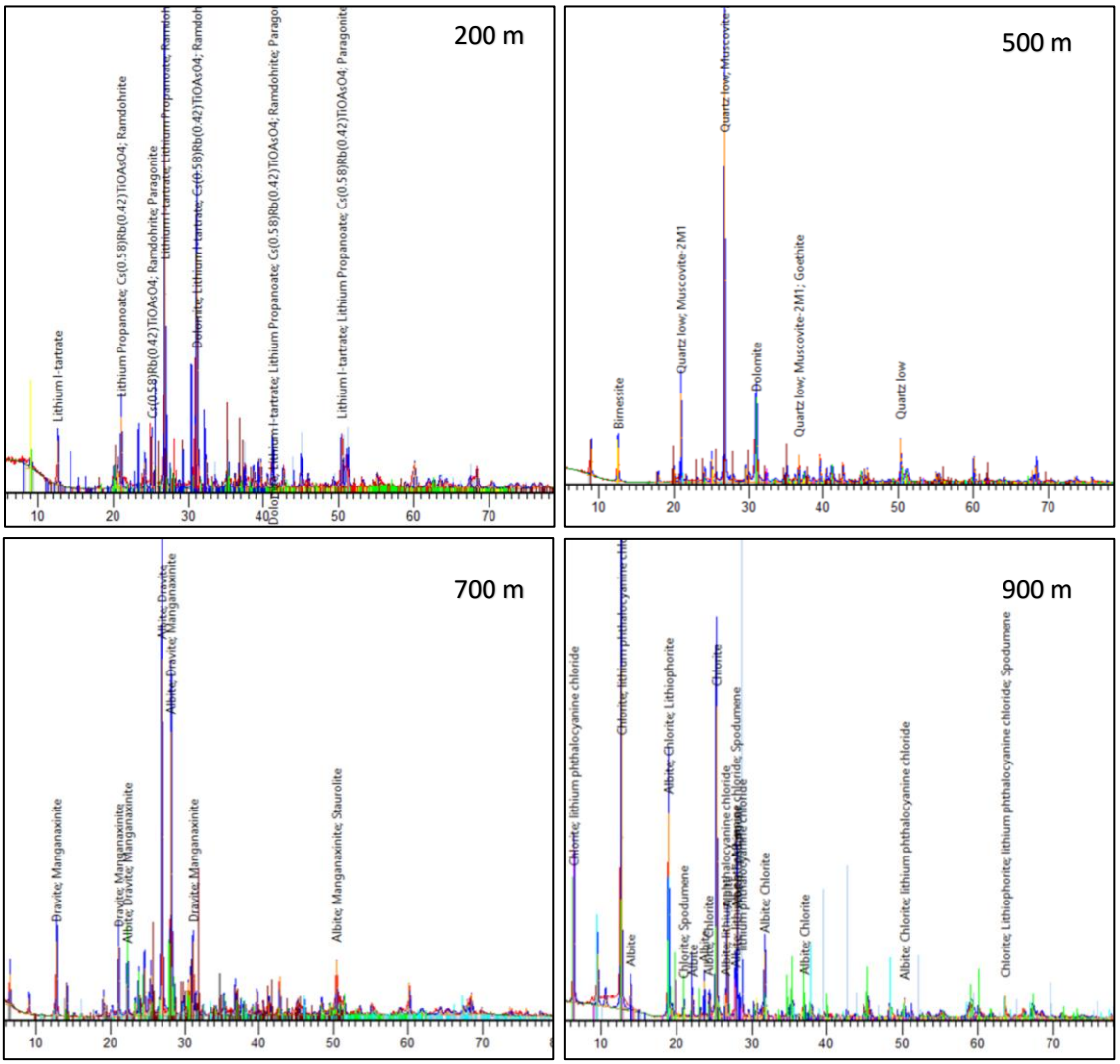


Figure 3. Mineralogical alterations at 200 m (a transition phase of Li transport prior to the precipitation of more stable Li silicates), 500 m (transition from deep K-metasomatic alteration to near-surface oxidative

precipitation), 700 m (transition formed under moderately high temperature, Na–B–Mn-rich, and oxidizing conditions), and 900 m (stage where Li is transported from deep magmatic fluids to surface oxidative and organic environments, being retained during this process by Na metasomatism, Fe–Mg alteration, and Mn-oxide precipitation). The XRD patterns correspond to these stages.

Acknowledgements

This study has received funding by the European Union Horizon research and innovation programme under Grant agreement No 101058163 (CRM-geothermal).

REFERENCES

Ayzit, T., Erol, S., Baba, A., 2025. Petrogenesis and comprehensive thermal assessment of the Dikili-Bergama region, western Anatolia. Geothermics 129, 103306. https://doi.org/https://doi.org/10.1016/j.geothermics.2025.103306

Benson, T.R., Coble, M.A., Dilles, J.H., 2023. Hydrothermal Enrichment of Lithium in Intracaldera Illite-Bearing Claystones. Sci. Adv. https://doi.org/10.1126/sciadv.adh8183

Chen, J.-Z., Zhang, H., Tang, Y., Lv, Z.-H., An, Y., Wang, M.-T., Liu, K., Xu, Y.-S., 2022. Lithium mineralization during evolution of a magmatic–hydrothermal system: Mineralogical evidence from Li-mineralized pegmatites in Altai, NW China. Ore Geol. Rev. 149, 105058. https://doi.org/https://doi.org/10.1016/j.oregeorev.2022.105058

Dini, A., Lattanzi, P., Ruggieri, G., Trumpy, E., 2022. Lithium Occurrence in Italy—An Overview. Minerals. https://doi.org/10.3390/min12080945

Ettehadi, A., Chuprin, M., Mokhtari, M., Gang, D.D., Wortman, P., Heydari, E., 2024. Geological Insights Into Exploration and Extraction of Lithium From Oilfield Produced-Water in the USA: A Review. Energy \& Fuels. https://doi.org/10.1021/acs.energyfuels.4c00732

Friðleifsson, G.Ó., Elders, W.A., Zierenberg, R.A., Fowler, A., Weisenberger, T.B., Mesfin, K.G., Sigurðsson, Ó., Níelsson, S., Einarsson, G.M., Óskarsson, F., Guðnason, E.Á., Tulinius, H., Hokstad, K., Gibert, B., Nono, F., Loggia, D., Parat, F., Cichy, S.B., Escobedo, D., Mainprice, D., 2020. The Iceland Deep Drilling Project at Reykjanes: Drilling Into the Root Zone of a Black Smoker Analog. J. Volcanol. Geotherm. Res. https://doi.org/10.1016/j.jvolgeores.2018.08.013

Gourcerol, B., Sanjuan, B., Millot, R., Rettenmaier, D., Jeandel, E., Genter, A., Bosia, C., Rombaut, A., 2024. Atlas of lithium geothermal fluids in Europe. Geothermics 119, 102956. https://doi.org/https://doi.org/10.1016/j.geothermics.2024.102956

Icenhower, J., London, D., 1996. No Title. Am. Mineral. 81, 719–734. https://doi.org/doi:10.2138/am-1996-5-619

Konrad-Schmolke, M., Halama, R., 2014. Combined Thermodynamic–geochemical Modeling in Metamorphic Geology: Boron as Tracer of Fluid–rock Interaction. Lithos. https://doi.org/10.1016/j.lithos.2014.09.021

Okay, A.I., Tüysüz, O., 1999. Tethyan sutures of northern Turkey. Geol. Soc. London, Spec. Publ. 156, 475–515.

Rosen, M.R., Stillings, L.L., Kane, T., Campbell, K.M., Vitale, M. V, Spanjers, R.P., 2020. Li and Ca Enrichment in the Bristol Dry Lake Brine Compared to Brines From Cadiz and Danby Dry Lakes, Barstow-Bristol Trough, California, USA. Minerals. https://doi.org/10.3390/min10030284

Serpen, U., Aksoy, N., Öngür, T., Korkmaz, E.D., 2009. Geothermal Energy in Turkey: 2008 Update. Geothermics. https://doi.org/10.1016/j.geothermics.2009.01.002